Journal of Applied Polymer Science

A highly selective polybenzimidazole-4,4′-(hexafluoroisopropylidene)bis(benzoic acid) membrane for high-temperature hydrogen separation

Sun Hee Choi,[1] Da Hye Kim,[1,2] Do Young Kim,[1,2] Jun Young Han,[1] Chang Won Yoon,[1,3] Hyung Chul Ham,[1] Jin-Ho Kim,[4] Hyoung-Juhn Kim,[1] Suk Woo Nam,[1,2] Tae-Hoon Lim,[1,2] Jonghee Han[1,2]

[1]Fuel Cell Research Center, Korea Institute of Science and Technology, 39-1 Hawolgok-dong, Sungbuk-gu, Seoul 136-791, Republic of Korea

[2]Green School, Korea University, 145 Anam-ro, Seongbuk-gu, Seoul 136-791, Republic of Korea

[3]Department of Clean Energy and Chemical Engineering, Korea University of Science and Technology, Republic of Korea

[4]Youlchon chemical, 78 Beomjigi-ro, Danwon-gu, Ansan-si, Gyeonggi-do 425-851, Republic of Korea

Correspondence to: S. H. Choi (E-mail: shchoi@kist.re.kr) and J. Han (E-mail: jhan@kist.re.kr)

ABSTRACT: A polymeric gas separation membrane utilizing polybenzimidazole based on 4,4′-(hexafluoroisopropylidene)bis(benzoic acid) was prepared. The synthesized membrane has an effective permeating area of 8.3 cm^2 and a thickness of 30 ± 2 μm. Gas permeation properties of the membrane were determined using H_2, CO_2, CO, and N_2 at temperatures ranging from 24°C to 200°C. The PBI-HFA membranes not only exhibited excellent H_2 permeability, but it also displayed superior gas separation performance particularly for H_2/N_2 and H_2/CO_2. The permeation parameters for both permeability and selectivity [P_{H_2} and $\alpha(H_2/N_2)$; P_{H_2} and $\alpha(H_2/CO_2)$] obtained for the new material were found to be dependent on trans-membrane pressure difference as well as temperature, and were found to surpass those reported by Robeson in 2008. © 2015 Wiley Periodicals, Inc. J. Appl. Polym. Sci. **2015**, *132*, 42371.

KEYWORDS: membranes; properties and characterization; separation techniques

Received 16 January 2015; accepted 14 April 2015
DOI: 10.1002/app.42371

INTRODUCTION

Owing to the growing need for H_2 purification and CO_2 capture in industrial applications such as syngas processing, integrated gasification combined cycle (IGCC) processes, power production, and hydrogen recovery, H_2-selective membranes have attracted significant research attention. To date, commercially available hydrogen has been produced predominantly from steam reforming using fossil fuels, such as natural gas, oil, and coal, as the reactor feed.[1,2] Unfortunately, CO_2 is the main by-product in these processes and needs to be captured in order to produce high purity hydrogen, as well as to lessen contribution to the greenhouse effect. For these reasons, significant efforts have been made to develop an efficient H_2/CO_2 separation technology based on H_2-selective membranes.

One approach is to utilize polymeric membranes that consist of organic materials, owing to their low cost, synthetic feasibility, mechanical flexibility, processability, and scalability.[3–5] In polymeric membranes, gas permeation is controlled by the solution-diffusion mechanism[6] in which gas pair selectivity is the product of diffusion selectivity and solubility selectivity. A polymeric membrane tends to selectively transport small gas molecules (e.g., H_2, kinetic diameter: 2.89 Å) but may be permeated by condensable gases (e.g., CO_2, kinetic diameter: 3.30 Å) with high solubility selectivity.[7] Since the diffusion selectivity and solubility selectivity for H_2 and CO_2 transports follow opposite trends, the separation of H_2 and CO_2 is particularly complicated and challenging compared to that of other gas pairs. For this reason, H_2-selective membranes for H_2/CO_2 separation are often made from glassy polymers because they can improve the overall permeation selectivity by selectively driving H_2 permeability. The separation performance of glassy polymers, however, can be severely deteriorated by CO_2-induced plasticization.[8,9]

A heterocyclic polymer, polybenzimidazole (PBI), has recently been recognized as an alternative for the desired gas separation because of its high thermal stability,[10] excellent mechanical properties, chemical stability, and high intrinsic H_2/CO_2 selectivity. Moreover, this type of polymer has an extremely rigid structure as evidenced by its high T_g,[11] which may provide high resistance

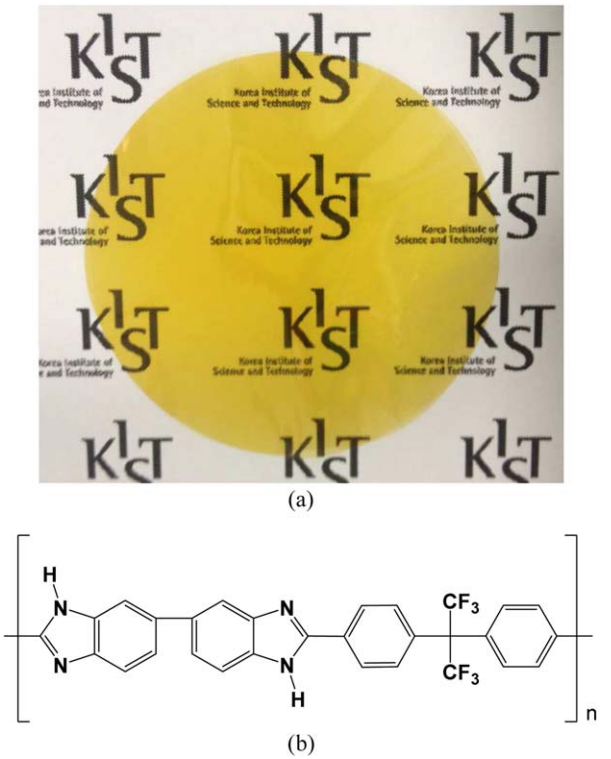

Figure 1. (a) Image of the PBI-HFA membrane and (b) structure for the repeat unit of PBI-HFA. [Color figure can be viewed in the online issue, which is available at wileyonlinelibrary.com.]

against CO_2 plasticization, allowing it to maintain its separation performance even at elevated temperatures. Despite these advantages, PBI polymers have major drawbacks for gas separation. These are (i) low H_2 permeability resulting from the rigid polymeric backbone and high degree of chain packing and (ii) brittleness, making it difficult to fabricate an ultrathin film from this material.[12] Several strategies, including polymer blending,[13] replacement of the PBI acid moiety,[11] chemical cross-linking,[14] thermal rearrangement of a precursor polymer,[15] modifications with *N*-substitution,[16] and incorporation of inorganic particles,[17,18] have been proposed to overcome these drawbacks. Of these, substitution of the PBI acid moiety with a dibenzoic acid monomer appears to be viable since the structural modification of the PBI polymer would suppress chain packing while simultaneously preventing chain mobility, affording an enhanced gas permeability with an increased selectivity.[19–21]

Recently, the structural alteration of PBI with the hexafluoroisopropylidine (HFA) group was reported to loosen its chain packing as well as to enhance the gas permeation properties of various polymers.[11,22,23] The substituted PBI polymer showed a higher density (1.34 g cm^{-3}) than other glassy polymers,[24] suggesting a closer chain packing in the PBI. A possible strategy could be to combine bulky groups that enhance free volume without severely affecting chain/subgroup rigidity, so that gas permeability can be improved.

In this article, we report efficient PBI based polymeric membranes for gas separation. The polymeric membranes, structurally perturbed with an HFA moiety through the PBI backbone (PBI-HFA), proved to have enhanced H_2 permeability combined with a superior permselectivity for H_2/N_2 and H_2/CO_2. Controlling factors for increasing gas permeability were further identified.

Synthesis of PBI Polymer

In a typical experiment, 4,4′-(hexafluoroisopropylidene)bis(benzoic acid) (HFA, 21.96 g) and 3,3′-diaminobenzidine (DAB, 12 g) were dried at 60°C under vacuum for 3–4 d. The dried mixture of HFA and DAB was stirred in a round bottom flask at 100°C for 40 min under Ar using a mechanical stirrer, followed by the addition of polyphosphoric acid (600 g). The resulting mixture was heated at 150°C for 12 h while stirring, and then the temperature was slowly increased to 220°C with continuous stirring for 5 h, affording highly viscous, yellow brownish polymeric mixtures. After the reaction mixture was poured into water, fibrous polymers were formed. The precipitated polymers were washed with distilled water at 60°C, followed by filtration. This process was repeated several times. To remove residual phosphoric acid, the polymer was washed with potassium hydroxide (1*M*) at 60°C for 2 d, followed by filtration and several washes with distilled water. The washed polymers were dried in a vacuum oven preheated to 100°C to yield PBI-HFA.

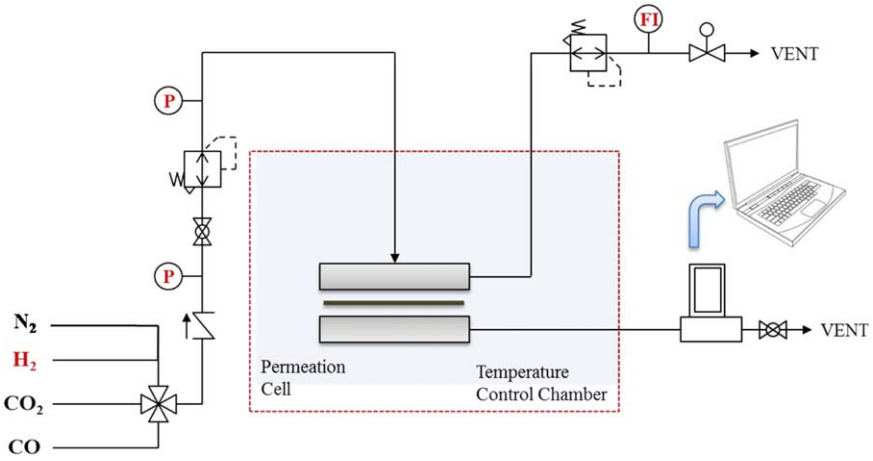

Figure 2. Schematic diagram of the high-temperature gas permeation setup. [Color figure can be viewed in the online issue, which is available at wileyonlinelibrary.com.]

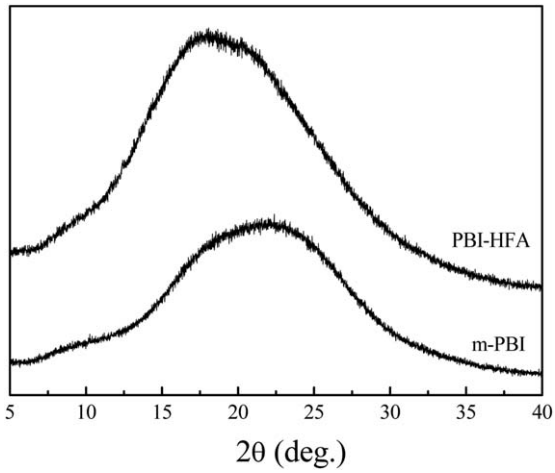

Figure 3. Wide angle X-ray diffraction spectra of m-PBI and PBI-HFA.

Preparation and Characteristics of PBI-HFA Membranes

PBI-HFA based membranes were prepared by dissolving the dried PBI-HFA polymer (0.18 g) in N-methyl-2-pyrrolidone (NMP, 9 g) at 60°C. The resulting solution was filtered using a 0.45 μm polytetrafluoroethylene (PTFE) syringe filter and then transferred to a glass dish where it formed a uniform, thin covering. This solution was then dried in a vacuum oven preheated to 60°C for 3 d followed by additional drying at 80°C to remove residual NMP. The dried PBI-HFA membranes were peeled from the glass dish using distilled water and then soaked in methanol for 1 h. The PBI-HFA membranes were then dried in a vacuum oven at 60°C for 1 d, ultimately affording the desired gas separation membranes in a disk shape with a diameter of 47 mm and a thickness of 30 ± 2 μm [Figure 1(a)]. The chemical structures of the repeat unit of PBI-HFA are shown in Figure 1(b). The wide angle X-ray diffraction (WAXD) spectrum of PBI-HFA in a film form was recorded using a Rigaku X-ray diffractometer (D/max 2500/PC) with Cu Kα1 radiation at 40 kV and 200 mA in a 2θ range of 5–40°. The average d-spacing (d_{sp}) was then calculated using Bragg's equation. The functional groups in the PBI-HFA membranes were characterized using an attenuated total reflection-Fourier transform infrared (ATR-FTIR) spectrometer (IS-10, Thermo) with a scan range from 4000 to 650 cm^{-1}. The PBI-HFA structure was further studied using ^1H NMR spectroscopy (Bruker, 300 MHz).

Densities of the membranes were measured using a Satorius Cubis MSA analytical balance (Satorius mechatronics, Germany) with a density kit based on Archimedes' principle. The obtained densities were used to derive fractional free volumes (FFV), Vf, of the polymers with the following equation:

$$V_f = \frac{V_{sp} - 1.3V_W}{V_{sp}} \quad (1)$$

where V_{sp} is the specific molar volume of the repeating unit of the polymers derived from the molecular weight of repeating unit by density, and V_W is the van der Waals volume of the repeating unit based on Bondi's group contribution approach.[25] The temperature-dependent dynamic mechanical properties of m-PBI and PBI-HFA films were measured using a dynamic mechanical analyzer (DMA) (TA Instruments, model Q-800). The dimensions of the films were 12.7 mm × 5.3 mm × 0.025 mm ($L \times W \times T$), and the films were cut and clamped on a film tension clamp in a precalibrated instrument. The samples were scanned from room temperature to 200°C at a heating rate of 10°C/min. The storage modulus (E'), loss modulus (E''), and tan δ values were determined at a constant linear frequency of 1 Hz with a preload force 0.01 N.

Evaluation of the water uptake of the membranes was also carried out to evaluate the stability of the membranes. The prepared m-PBI and PBI-HFA membrane samples were immersed in aqueous solutions at room temperature and 80°C for 24 h. After water uptake, the residual water in the surfaces of the samples was removed by an absorption paper. The water uptake of the membranes were then recorded and calculated using the following equation:

$$\text{Wateruptake}(\%) = \frac{W_{wet} - W_{dry}}{W_{dry}} \quad (2)$$

where W_{wet} is the weight of the fully water-absorbed membrane, and W_{dry} the weight of the dry membrane. The molecular weights of m-PBI and PBI-HFA polymer were determined by gel permeation chromatography (GPC) using a Waters GPC system. The column was filled with 2× TSKgel α-M (7.8 × 300 mm) and NMP with the addition of 0.01M LiBr was used as the eluent. The eluent pumping rate (Waters 515) was 0.5 mL/min and the temperature was 45°C. Polystyrene was used as the standard. Detection was accomplished using a Waters 410 differential refractometer.

Determination of Gas Permeability

Permeation experiments utilizing pure gas were performed by a high-temperature gas permeation set-up, as depicted in Figure 2. In a typical experiment, a single gas regulated by a needle valve was fed into the polymer membrane and the permeated gas flux was determined using a bubble flow meter. The pressure of the feed gas was controlled by a back-pressure regulator. The permeation fluxes of H_2, N_2, CO_2, and CO (99.9% purity) were measured at various temperatures ranging from 24°C to 200°C. Operating pressures from 0.4 to 0.8 MPa were controlled

Table I. Physical Properties of PBI-HFA and m-PBI Membranes at 24°C

	M_W (g/mol)	V_{sp} (cm^3/mol)	Density (g/cm^3)	V_W (cm^3/mol)	V_f	d-spacing (Å)
PBI-HFA	578.56	426.35	1.357	249.1	0.240	4.907
m-PBI	338.41	261.32	1.295	159.8	0.205	4.04

[a] M_W: molecular weight of repeating unit, $Vf = (V_{sp} - 1.3V_W)/V_{sp}$ (Vf: fractional free volume; V_W: van der Waals volume; V_{sp}: specific molar volume). V_W was calculated using Bondi's group contribution approach.[25]

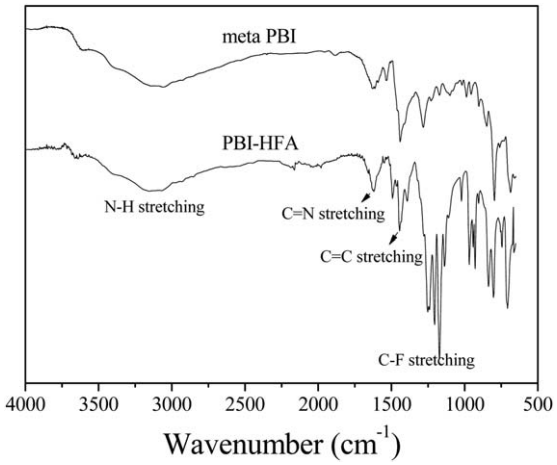

Figure 4. FT-IR spectra of m-PBI and PBI-HFA.

using a pressure regulator in all permeation tests. The effective permeating area of the prepared membrane was 8.3 cm^2.

In general, gas permeation through a nonporous polymeric membrane is known to occur via the solution-diffusion mechanism[26] in which gas pair selectivity is the product of diffusion selectivity and solubility selectivity. Gas molecules initially diffuse from the feed side of a polymeric membrane into the surface of the membrane where they start dissolving. The dissolved molecules then permeate through the spaces between the polymer chains of the membrane by random molecular diffusion, followed by desorption and diffusion to the permeate side. The gas permeability (P) is calculated using the following formula:

$$P = \frac{273 \times QL}{AT\Delta P} \quad (3)$$

where P refers to the membrane gas permeability in Barrer (1 Barrer = 1×10^{-10} cm^3(STP) cm cm^{-2} s^{-1} $cmHg^{-1}$, Q is the volumetric flow rate of gas (cm^3(STP)/s), L represents the membrane thickness (cm), A is the effective membrane area (cm^2), T indicates the operating temperature (K), and ΔP is the transmembrane pressure difference (cmHg). The ideal permselectivity, $\alpha(H_2/CO_2)$, of a membrane for H_2 and CO_2 gas pair is given as

$$\alpha(A/B) = P_A/P_B \quad (4)$$

where A = H_2 and B = CO_2

RESULTS AND DISCUSSION

Because of its bulky nature, the HFA group's presence in the PBI-HFA membrane is known to result in increased d-spacing compared to that of unsubstituted analogs.[20] Since PBI-HFA polymer with large d-spacing and inner pores could show enhanced gas permeability, we initially determined the d-spacing of the as-prepared PBI-HFA polymer in the film form using wide-angle X-ray diffraction (WAXD). The obtained spectra showed broad peaks (Figure 3), indicating that the m-PBI and PBI-HFA polymers are highly amorphous in nature. The details on the fabrication of m-PBI membranes were described in our previous article.[27] On the basis of this result, Bragg's equation, $n\lambda = 2\ d_{sp}\sin(\theta)$, gave a polymer d-spacing (d_{sp}) of 4.04 and 4.907 Å for m-PBI and PBI-HFA, respectively. The peak position of PBI-HFA was found to appear at a lower angle than m-PBI, indicating decreased polymer chain packing. The increased d-spacing of PBI-HFA is expected to increase as a result of the FFV and the gas permeability.

Glassy polymers have different types of free volume, and the diffusion mechanism in glassy polymer membranes will depend on the nature of the free volume and the polymer backbone chain flexibility. In many cases, the disruption of a rigid structure with well-packed chains increases the free-volume fraction and weakens intermolecular interactions. As shown in Table I, based on density data, we estimated the fractional free volume (V_f) of m-PBI and PBi-HFA membranes. The obtained free volume, d-spacing, and relevant data are listed in Table I. The V_f is a major physical determinant for the transport of small molecules in polymers. The calculated V_f of PBI-HFA membrane (0.240) was found to be higher than that of m-PBI membrane (0.205), which is consistent with the increased gas permeability of PBI-HFA compared to that of m-PBI membrane. This trend is also in good agreement with the change in average d-spacing that is associated with the amount of available space for small molecule transport through a polymer

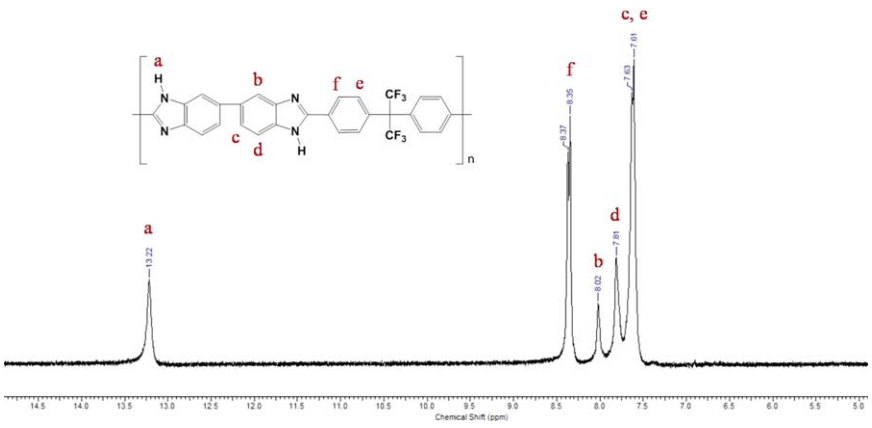

Figure 5. ^{1}H-NMR (300 MHz, DMSO-d_6) spectra of the PBI-HFA. [Color figure can be viewed in the online issue, which is available at wileyonlinelibrary.com.]

Table II. Pure Gas Separation Performance of PBI-HFA and m-PBI at 24°C and 8 kgf/cm^2

	$P(H_2)^a$	$P(N_2)^a$	$P(CO_2)^a$	$P(CO)^a$	$\alpha(H_2/N_2)$	$\alpha(H_2/CO_2)$	$\alpha(H_2/CO)$	$\alpha(CO_2/N_2)$
PBI-HFA	121.3	1.47	50.1	2.8	82.5	2.4	43.3	34.1
m-PBI	1.48	0	0	0	∞	∞	∞	-

[a] Expressed in Barrer (1 Barrer = 1×10^{-10} cm^3(STP) cm cm^{-2} s^{-1} cmHg^{-1}).

membrane. Obviously, the increased fractional free volume and large average d-spacing in PBI-HFA membrane explain the improved gas permeability.

Consistent with the previous results,[22] the as-synthesized PBI-HFA polymer characterized by FT-IR spectroscopy exhibited the characteristic C═C and C═N stretching frequencies of the benzimidazole ring at 1440, 1600, and 1620 cm^{-1} (Figure 4).[28] The characteristic peaks for N—H stretching were also observed in the range 2800–3500 cm^{-1}. Furthermore, an additional broad band corresponding to C—F stretching vibrations appeared in the range 1155–1258 cm^{-1} in comparison with m-PBI.[22] This polymer was then analyzed using ^{1}H NMR spectroscopy following dissolution in DMSO-d_6 (Figure 5). The signal for the proton attached to the nitrogen of the imidazole group was observed at $\delta = \sim 13.2$. In addition, signals for the aromatic protons at $\delta = 7.5$–8.5 were also observed.

To investigate the gas permeation properties of the as-synthesized polymer, we prepared the PBI-HFA membranes using a solution casting method. The resulting membranes were then used to determine gas permeability using H_2, N_2, CO_2, and CO. Table II summarizes the single-gas permeability and ideal selectivity determined at 24°C and 8 kgf/cm^2 using PBI-HFA and m-PBI membranes with a thickness of 30 ± 2 μm. The effective permeating area of the prepared membranes was calculated to be 8.3 cm^2. The permeability was found to decrease in the order of $H_2 > CO_2 > CO > N_2$, which is in general agreement with previous results employing PBI membrane derivatives.[11] Gas permeabilities of PBI membranes correlated well with the kinetic diameters of the gas molecules: H_2 (2.89 Å) < CO_2 (3.30 Å) < N_2 (3.64 Å). This result indicates that a diffusion-based selectivity (or size sieving effect) played a dominant role in the gas transport properties. The CO permeability was not compared in this study because, to the best of our knowledge, studies for CO permeability across the PBI membrane have not been previously reported.

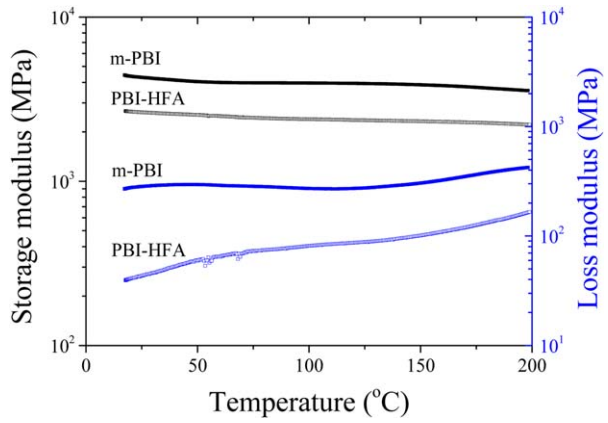

Figure 6. Storage modulus (E') and loss modulus (E'') against temperature plots of m-PBI and PBI-HFA polymers. [Color figure can be viewed in the online issue, which is available at wileyonlinelibrary.com.]

M-PBI has not been considered as a viable material for H_2 separation because of its low permeability,[29] which is attributed to its tight and close chain packing characteristics caused by strong pi-pi interactions and hydrogen bonding among polymer chains. The temperature-dependent thermo-mechanical properties, such as storage modulus (E'), loss modulus (E'') and tan δ of the m-PBI and PBI-HFA polymers, were determined using DMA. The change in the functionality of a polymer can alter the results obtained from DMA. The storage modulus is associated with the stiffness of a material, and the dynamic loss modulus is often associated with its internal friction. As shown in Figure 6, the storage modulus and dynamic loss modulus of m-PBI is larger than those of PBI-HFA. This increases in moduli can be manifested in the decrease in free volume, leading to an increase in mechanical relaxation time.[30] Therefore, lower values of the moduli in PBI-HFA also explain its higher gas permeability. The water uptake abilities of m-PBI and PBI-HFA membranes were further evaluated because water molecules are included in combustion gases. As given in Table III, the m-PBI membrane shows higher water uptake compared to the PBI-HFA membrane. In all the cases except CO_2, the measured gas permeances decrease as the humidity in the feed increases, implying that the condensed water molecules in the membranes hinder the transport of noncondensable small gas molecules.[31] Therefore, m-PBI is expected to show a larger decrease in H_2 permeance than PBI-HFA as the humidity of the feed increases.

Compared to those of the previously reported PBI, the gas permeability values using our PBI-HFA membranes are significantly increased, presumably owing to the decreased packing density resulting from the incorporation of HFA in the PBI backbone. In addition, the decrease in N—H group density upon structural modification of PBI with HFA potentially reduces intermolecular hydrogen bonding interactions,

Table III. Water Uptake of the Fabricated m-PBI and PBI-HFA Membranes

	21°C	90°C
PBI-HFA	14.1%	10.6%
m-PBI	25%	18.1%

Thickness: 30 μm, area: 8.3 cm^2.

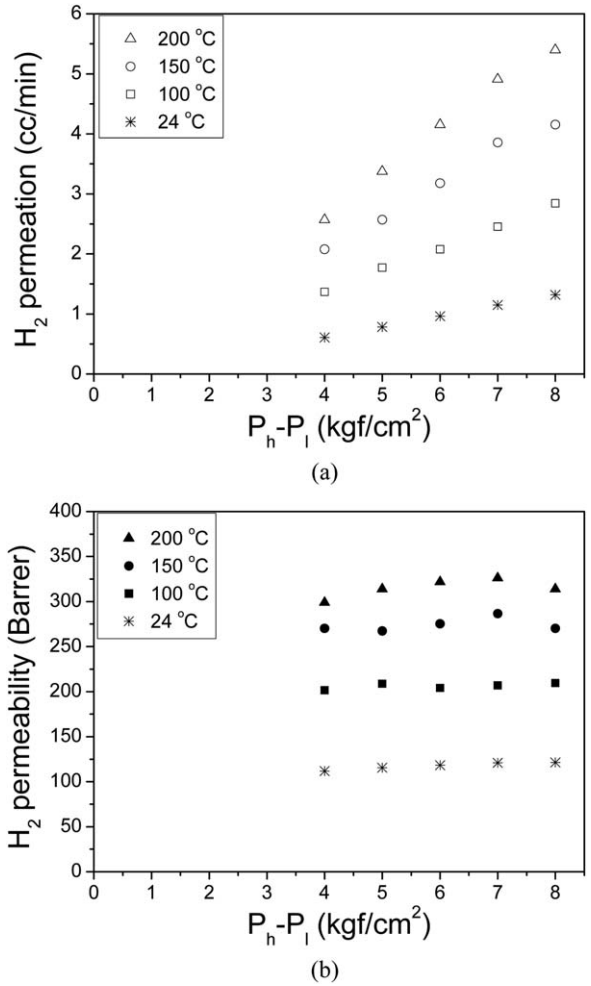

Figure 7. (a) Variation of H_2 permeation and (b) H_2 permeability with pressure.

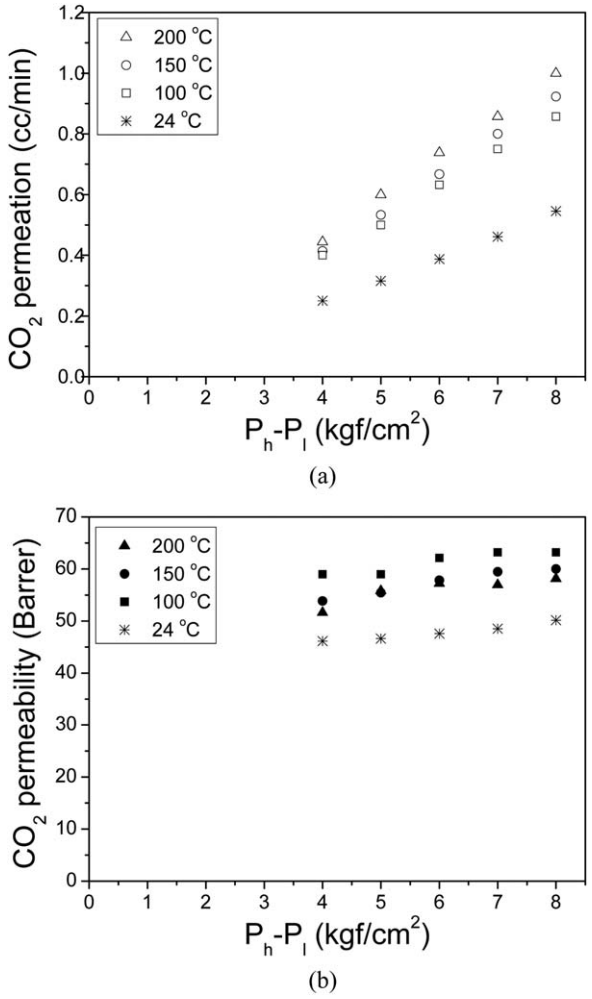

Figure 8. (a) Variation of CO_2 permeation and (b) CO_2 permeability with pressure.

increasing free volume in the polymer matrix. Moreover, the HFA group allows additional flexibility around the bridge carbon.

The H_2 permeation through the as-prepared membranes was further measured as a function of pressure difference using pure H_2 gas from 24°C to 200°C (Figure 7). At all temperatures, a higher hydrogen permeation is obtained at a higher pressure difference. In fact, the hydrogen permeation displayed a linear relationship with the pressure difference, suggesting that the rate-limiting step of the hydrogen permeation through the membrane is the diffusion of molecular hydrogen to and/or from the surface. The H_2 permeability is also found to increase as temperature increases [Figure 7(b)], which results from an increased H_2 diffusivity at higher temperatures. As shown in Figure 7(b), a virtually constant H_2 permeability as a function of pressure difference is observed, suggesting the absence of viscous flow and defects in the tested PBI-HFA membranes. To the best of our knowledge, the as-prepared PBI-HFA membranes show a higher H_2 permeability (121 Barrer at 24°C) than any other as-prepared PBI-HFA membranes reported in the literature.[10,11] Intrinsic gas permeability indicates an increasing trend with an increase in molecular weight. [32,33] These are in agreement with Kesting's hypothesis[34] that free volume of dense films increases with an increase in the molecular weight of the polymer. An increase in molecular weight causes an increase in chain entanglement, which may in turn result in an increase in chain stiffness leading to a decrease in packing density. As given in Table IV, the molecular weight of PBI-HFA (M_w: 164,000) is larger than that of m-PBI (M_w: 73,700). Therefore, the packing density of PBI-HFA membranes is expected to decrease, presumably because of the increased *d*-spacing of PBI-HFA (Figure 3), which further induces the increased free volume and gas

Table IV. Molecular Weights of the Fabricated m-PBI and PBI-HFA Membranes

	M_n[a]	M_w[b]	M_w/M_n
PBI-HFA	18,200	164,000	9.01
m-PBI	25,900	73,700	2.85

[a] Number average molecular weight.
[b] Weight average molecular weight.

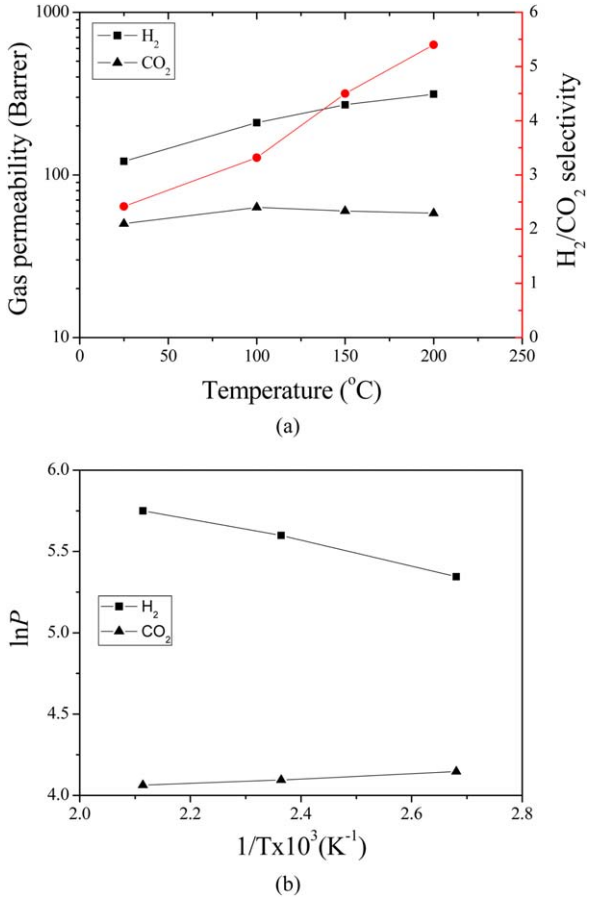

Figure 9. (a) H_2/CO_2 separation performance of PBI-HFA membrane at different temperatures, and (b) temperature dependence of gas permeability in the PBI-HFA membrane. [Color figure can be viewed in the online issue, which is available at wileyonlinelibrary.com.]

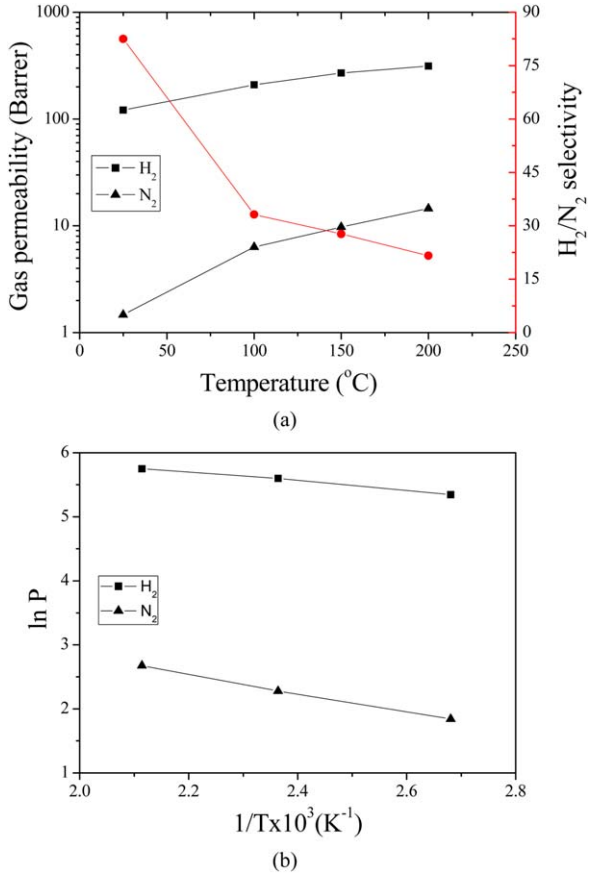

Figure 10. (a) H_2/N_2 separation performance of the PBI-HFA membrane at different temperatures, and (b) temperature dependence of gas permeability in the PBI-HFA membrane. [Color figure can be viewed in the online issue, which is available at wileyonlinelibrary.com.]

permeability (Tables I and II). Moreover, neither thermal rearrangement nor the incorporation of inorganic particles into the membrane has been attempted to increase H_2 permeability.

CO_2 permeation through the PBI-HFA membranes was also determined from 24°C to 200°C according to pressure differences (Figure 8). The CO_2 permeation is also found to increase as the CO_2 pressure difference increases [Figure 8(a)]. However, unlike in the case of H_2, the CO_2 permeability is inversely correlated with temperature [Figure 8(b)]; i.e., as temperature increases from 100°C through 150°C to 200°C, the CO_2 permeability decreases. Considering that a sorption process contributes to the transport of a condensable gas such as CO_2 through a polymer film with high solubility selectivity,[7] it seems logical that this phenomenon is caused by a significant drop in CO_2 sorption into the membrane surface at elevated temperatures.

On the basis of the results above, the H_2/CO_2 separation properties of the PBI-HFA membranes were obtained at different temperatures [Figure 9(a)]. Obviously, the H_2/CO_2 selectivity considerably increases with increasing temperature because the gas permeation of H_2 and CO_2 through the membranes exhibits quite different behaviors between the smaller gas molecule (H_2) and the relatively larger molecule (CO_2) at elevated temperatures. The permeability of each gas can further be correlated with the temperature through the van't Hoff-Arrhenius equation:[35]

$$P = P_o \exp\left(\frac{-E_P}{RT}\right) \quad (5)$$

where P is the gas permeability, P_o is the pre-exponential coefficient, E_p is the apparent activation energy for the permeation process, R is the gas constant, and T is the absolute temperature. A plot of ln$P$ *vs* $1/T$ using the van't Hoff equation afforded activation energies (E_p) of 6.0 and −1.2 kJ/mol, for H_2 and CO_2 permeation across the PBI-HFA membranes, respectively [Figure 9(b)]. The negative activation energy for CO_2 again indicates a decrease in CO_2 permeability as temperature increases.

The H_2/N_2 separation properties of the PBI-HFA membranes were obtained at different temperatures [Figure 10(a)]. The H_2 and N_2 permeabilities of PBI-HFA membranes are found to increase with temperature, indicating that the gas permeation follows a diffusion-dominated gas transport mechanism in the temperature range tested. Contrary to the H_2/CO_2 selectivity, the H_2/N_2 selectivity decreases considerably with increasing

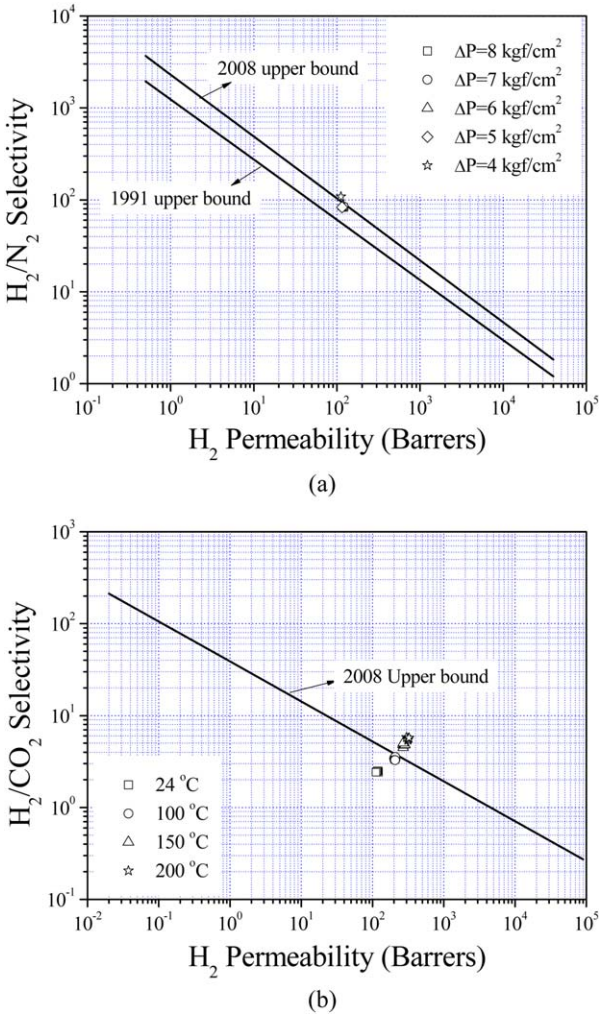

Figure 11. Robeson plot of (a) H_2/N_2 selectivity as a function of the H_2 permeability coefficient, and (b) H_2/CO_2 selectivity as a function of the H_2 permeability coefficient. [Color figure can be viewed in the online issue, which is available at wileyonlinelibrary.com.]

temperature, indicating that the permeability of N_2 increases more rapidly than that of H_2 as temperature increases. The selectivity of glassy polymers often decreases with increasing temperature because a less permeable gas component often possesses a higher activation energy: i.e., a less permeable gas undergoes a relatively larger increases in permeability upon increasing temperature. The temperature dependence of the ideal H_2/N_2 selectivity for PBI-HFA membranes follows this general trend. A plot of ln*P* *vs*1/*T*using the van't Hoff equation afforded an activation energy (*E*p) of 12.2 kJ/mol for N_2 permeation across the PBI-HFA membranes [Figure10(b)]. The activation energies for gas permeability (*E*p) were calculated to increase in the following order: $N_2 > H_2 > CO_2$. The results indicate the significant influence of temperature on N_2 permeability.

Figure 11 shows the relationship between gas permeability and gas selectivity of the as-synthesized PBI-HFA membranes by comparing the data for polymeric membranes reported by Robeson in 1991[36] and 2008.[37] Our PBI-HFA membranes showed outstanding gas separation performance with the mixture of H_2 and N_2 [Figure 11(a), rectangle], surpassing the 1991 upper bound as well as the 2008 upper bound for polymeric gas separation membranes. Moreover, the PBI-HFA membranes employed in this study further exhibited superior gas separation performance for the mixture of H_2 and CO_2, particularly at ≥ 150°C [Figure 11(b), triangle and asterisk], exceeding the 2008 upper bounds for polymeric gas separation membranes.[37] Very little data can be found in the literature for H_2/CO_2 separation at high temperature. The obtained H_2/CO_2 selectivity could be further improved by increasing the gas feeding temperature since the lowered CO_2 solubility at ≥ 200°C would lead to a drastic reduction of the CO_2 permeability of the PBI-HFA membranes. The improved permselectivities of the PBI-HFA membranes suggests their potential for H_2 separation from syngas at high temperatures.

CONCLUSIONS

In summary, the as-synthesized PBI-HFA membranes exhibited excellent gas permeation properties. The H_2 permeability of PBI-HFA determined at 24°C was found to be significantly higher than other gases. The linear relationship between the H_2 permeation fluxes and the trans-membrane H_2 pressure suggests that the diffusion of molecular hydrogen at the surface of the PBI-HFA membrane is the probable rate determining step for H_2 permeation. Except for CO_2, the gas permeability was found to increase as temperature increased, presumably because gas diffusivity increases with temperature. The different temperature dependences of H_2 and CO_2 behavior provided increased ideal permselectivity for H_2 and CO_2 with increased temperatures. The as-synthesized PBI-HFA membranes were shown to have outstanding gas separation performance for H_2/N_2 and H_2/CO_2, surpassing the 2008 upper bound suggested by Robeson. This membrane separation technology is thus applicable to the production of high purity hydrogen downstream of a number of reforming reactions.

ACKNOWLEDGMENTS

This work was supported by the Youlchon chemical and WPM funding.

REFERENCES

1. Ockwig, N. W.; Nenoff, T. M. *Chem. Rev.* **2007**, *107*, 4078.
2. Shao, L.; Low, B. T.; Chung, T. S.; Greenberg, A. R. *J. Membr. Sci.* **2009**, *327*, 18.
3. Stern, S. A. *J. Membr. Sci.* **1994**, *94*, 1.
4. Koros, W. J.; Fleming, G. K. *J. Membr. Sci.* **1993**, *83*, 1.
5. Baker, R. W. *Ind. Eng. Chem. Res.* **2002**, *41*, 1393.
6. Paul, D. R.; Yampol'skii, Y. P. Polymeric Gas Separation Membranes, 1st ed.; CRC Press: Boca Raton, **1994**.
7. Scgoles, C. A.; Kentish, S. E.; Stevens, G. W. *Sep. Purif. Rev.* **2009**, *38*, 1.
8. Bos, A.; Pünt, I. G. M.; Wessling, M.; Strathmann, H. *J. Membr. Sci.* **1999**, *155*, 67.

9. Chiou, J. S.; Paul, D. R. *J. Membr. Sci.* **1987**, *32*, 195.
10. Kumbharkar, S. C.; Islam, M. N.; Potrekar, R. A.; Kharul, U. K. *Polymer* **2009**, *50*, 1403.
11. Kumbharkar, S. C.; Karadkar, P. B.; Kharul, U. K. *J. Membr. Sci.* **2006**, *286*, 161.
12. Chung, T. S. *J. Macromol. Sci. Part C: Polym. Rev.* **1997**, *37*, 277.
13. Chung, T. S.; Xu, Z. L. *J. Membr. Sci.* **1998**, *147*, 35.
14. Hosseini, S. S.; Teoh, M. M.; Chung, T. S. *Polymer* **2008**, *49*, 1594.
15. Han, S. H.; Lee, J. E.; Lee, K. J.; Park, H. B.; Lee, Y. M. *J. Membr. Sci.* **2010**, *357*, 143.
16. Kumbharkar, S. C.; Kharul, U. K. *J. Membr. Sci.* **2010**, *357*, 134.
17. Sadeghi, M.; Semsarzadeh, M. A.; Moadel, H. *J. Membr. Sci.* **2009**, *331*, 21.
18. Yang, T.; Xiao, Y.; Chung, T. S. *Energy Environ. Sci.* **2011**, *4*, 4171.
19. Muruganandam, N.; Paul, D. R. *J. Membr. Sci.* **1987**, *34*, 185.
20. Hellums, M. W.; Koros, W. J.; Husk, G. R.; Paul, D. R. *J. Membr. Sci.* **1989**, *46*, 93.
21. Moe, M. B.; Koros, W. J.; Paul, D. R. *J. Polym. Sci. Part B: Polym. Phys.* **1988**, *26*, 1931.
22. Kumbharkar, S. C.; Liu, Y.; Li, K. *J. Membr. Sci.* **2011**, *375*, 231.
23. Hsu, S. L. C.; Lin, Y. C.; Tasi, T. Y.; Jheng, L. C.; Shen, C. H. *J. Appl. Polym. Sci.* **2013**, *130*, 4107.
24. Mecerreyes, D.; Grande, H.; Miguel, O.; Ochoteco, E.; Marcilla, R.; Cantero, I. *Chem. Mater.* **2004**, *16*, 604.
25. Bondi, A. *J. Phys. Chem.* **1964**, *68*, 441.
26. Scovazzo, P.; Kieft, J.; Finan, D. A.; Koval, C.; Dubois, D.; Noble, R. *J. Membr. Sci.* **2004**, *238*, 57.
27. Han, J. Y.; Lee, J. Y.; Kim, H. J.; Kim, M. H.; Han, S. G.; Jang, J. H.; Cho, E. A.; Yoo, S. J.; Henkensmeier, D. *J. Appl. Polym. Sci.* **2014**, *131*, 40521.
28. Musto, P.; Karasz, F. E.; MacKnight, W. J. *Polymer* **1993**, *34*, 2934.
29. Pesiri, D. R.; Jorgensen, B.; Dye, R. C. *J. Membr. Sci.* **2003**, *218*, 11.
30. Struik, L. C. E. Physical Ageing in Amorphous Polymers and Other Materials; Elsevier: Amsterdam, **1978**.
31. Kim, H. W.; Yoon, H. W.; Yoon, S. -M.; Yoo, B. M.; Ahn, B. K.; Cho, Y. H.; Shin, H. J.; Yang, H.; Paik, U.; Kwon, S.; Choi, J. -Y.; Park, H. B. *Science* **2013**, *342*, 91.
32. Eastmond, G. C.; Page, P. C. B.; Paprotny, J. *Polymer* **1993**, *34*, 667.
33. Chowdhury, G.; Vujosevic, R.; Matsuura, T.; Laverty, B. *J. Appl. Polym. Sci.* **2000**, *77*, 1137.
34. Kesting, R. E.; Fritzche, A. K. Polymeric Gas Separation Membranes; John Wiely & Sons: New York, **1993**.
35. Yampolskii, Y.; Pinnau, I.; Freeman, B. D. Materials Science of Membranes for Gas and Vapor Separation; John Wiley: Chichester, **2006**.
36. Robeson, L. M. *J. Membr. Sci.* **1991**, *62*, 165.
37. Robeson, L. M. *J. Membr. Sci.* **2008**, *320*, 390.